Vibrational density of states of general two-component random mixtures near percolation thresholds

1991 J. Phys.: Condens. Matter 3 4797

(http://iopscience.iop.org/0953-8984/3/26/003)

J. Phys.: Condens. Matter 3 (1991) 4797–4807. Printed in the UK

Vibrational density of states of general two-component random mixtures near percolation thresholds

Stefanie Russ, H Eduardo Roman and Armin Bunde

Institut für Theoretische Physik, Universität Hamburg, Jungiusstrasse 9, D-2000 Hamburg 36, Federal Republic of Germany

Received 19 October 1990, in final form 18 March 1991

Abstract. We study scalar vibrational properties of random networks where two types of harmonic springs, f_A and $f_B = hf_A$ ($h \ll 1$), are present with probability p and $1-p$, respectively. We develop a scaling theory for the density of states $N(\omega)$ near the critical concentration p_c, and test it by numerical simulations on the square lattice. For $p > p_c$ and h sufficiently small, we recover the standard fracton–phonon crossover at a characteristic frequency, determined by the correlation length ξ, $\omega_\xi \gg \omega_B$, where $\omega_B \sim f_B^{1/2}$ is the maximum frequency of the B sublattice. For finite h and p sufficiently close to p_c, we obtain a new type of fracton–phonon crossover determined by two characteristic frequencies: ω_h (which depends on h) and ω_B, with $\omega_h \ll \omega_B$. In this case, a hump mediates the crossover from fracton-like modes (occurring for $\omega \gg \omega_B$), to Debye phonons (occurring for $\omega \ll \omega_h$) when $\omega_h \gg \omega_\xi$.

1. Introduction

Vibrational properties of random two-component systems have been studied intensively in the past [1]. Typical examples are random alloys of two atomic species of arbitrary mass ratio and composition. It is well known that the density of vibrational states of those alloys is quite rich, and has a complex structure at intermediate compositions due to the existence of localized and extended modes in the frequency spectrum [1].

To some extent, two-component mixtures can be modelled by percolation networks in which all lattice sites are occupied by unit masses, and nearest-neighbor sites are connected by springs with force constants taking values $f_A = 1$ with probability p, and $f_B = hf_A$ with probability $1-p$ ($h < 1$). Above a critical concentration p_c, there exists an 'infinite' cluster of A bonds. The mean linear size ξ of the finite A clusters in the network represents a characteristic length scale in the system. On length scales r smaller than ξ, both the infinite cluster and the finite A clusters are self-similar and described by the fractal dimension d_f. On length scales larger than ξ, the infinite cluster is compact and described by the Euclidean dimension d of the network. The correlation length ξ diverges as $\xi \sim |p-p_c|^{-\nu}$ if p_c is approached [2].

So far, the vibrational properties of two-component networks near p_c have been studied only for the limiting case $h = 0$. In this case, ξ is the only characteristic length in the system, and determines a characteristic frequency ω_ξ for the vibrational modes. By exploiting the analogy between scalar vibrations and the corresponding random walk problem defined on the same percolation network, it has been shown

0953-8984/91/264797+11$03.50

that $\omega_\xi \sim \xi^{-d_w/2} \sim (p - p_c)^{\nu d_w/2}$ [3]. Here d_w characterizes the time evolution of the root-mean-square displacement (RMSD) $R(t) \sim t^{1/d_w}$ of random walks on the infinite A cluster at p_c [4,5], $d_w > 2$. For frequencies $\omega > \omega_\xi$ corresponding to length scales smaller than ξ, vibrations are strongly localized in space with a frequency-dependent localization length λ. These modes are called 'fractons' and can occur either on a portion of the infinite cluster or on finite A clusters whose linear size $L \gg \lambda$ [6]. For $\omega < \omega_\xi$, the vibrational modes extend over macroscopic length scales and correspond to sound waves.

The density of vibrational states $N(\omega)$ reflects the two regimes described above. For fractons one finds,

$$N(\omega) \sim \omega^{d_s'-1} \qquad \omega \gg \omega_\xi \tag{1.1}$$

where $d_s' = 2d/d_w$ is the spectral dimension [6], while for sound waves one has, as usual,

$$N(\omega) \sim \omega^{d-1} \qquad \omega \ll \omega_\xi. \tag{1.2}$$

This simple percolation model contains already the essential ingredients for describing the vibrational properties of several random fractal structures. Prominent examples are silica aerogels, which are self similar over a wide range of length scales [7, 8]. However, owing to the restrictive assumption $f_B = 0$, this model does not apply to random AB alloys in general. In ternary glassy compounds such as $Fe_xNi_xB_{1-2x}$ [10] essentially two types of bond strengths between the atoms seem to determine the vibrational properties of the system, and a similar picture may apply also to more complex systems such as $(AgI)_x(Ag_2O{\cdot}B_2O_3)_{1-x}$ glasses [11].

The purpose of this paper is to release the restrictive condition $h = 0$ and to study random two-component mixtures near the percolation threshold for the more general case $0 < h \ll 1$. For simplicity, scalar force constants are assumed. Our approach is based on the analysis of the probability of return to the origin, and has the advantage that it can be easily applied to both the $h = 0$ and $h > 0$ cases. To illustrate of this approach, which is simpler than those known in the literature [6, 12], we start with the standard percolation problem, $h = 0$.

2. Standard percolation networks

According to Alexander and Orbach [3] (see also [13]), the density of vibrational states $N(\omega)$ is related to the probability of return to the origin $P_0(t)$ in the corresponding random walk problem,

$$P_0(t) = \int_0^\infty d\omega\ N(\omega)\ \exp(-\omega^2 t). \tag{2.1}$$

To obtain $N(\omega)$, we calculate first $P_0(t)$. In the random walk problem, a random walker ('ant') is allowed to move along A bonds only, and can start its walk at a site belonging to any A cluster in the network. In order to obtain $P_0(t)$ one must average over all A clusters in the system.

First we consider random walks at p_c, on the restricted ensemble of A clusters with the same (fixed) number of sites s. The mean probability of being at those sites where the ants started, $P_0^{(s)}(t)$, is proportional to the inverse of the mean number of sites explored by the ants, i.e. $P_0^{(s)}(t) \sim [R_s(t)]^{-d_t}$, where $R_s(t) \sim t^{1/d_w}$ for $t < s^{d_w/d_t}$, and $R_s(t) \sim s^{1/d_t}$ for $t > s^{d_w/d_t}$ [5]. Since the probability that an A cluster of s sites occurs in the network scales as s^{-d/d_t} [2], we obtain $P_0(t)$ by averaging over all cluster sizes s,

$$P_0(t) \sim \sum_{s=1}^{\infty} s^{-d/d_t} P_0^{(s)}(t) \qquad p = p_c.$$

To obtain $P_0(t)$, we follow a procedure employed in [5] to calculate the root-mean-square displacement $R(t)$. Due to the presence of finite A clusters in the network, $P_0(t)$ tends to a (p-dependent) constant $P_0(\infty)$ at large times, and we find

$$P_0(t) - P_0(\infty) \sim t^{-d_s'/2} \tag{2.2}$$

where $d_s' = 2d/d_w$, $d_s' \cong 1.39$ in two dimensions. If we consider diffusion on the infinite cluster alone, $P_0(\infty) = 0$ and $P_0(t)$ scales as $P_0(t) \sim [R(t)]^{-d_t} \sim t^{-d_t/d_w}$. In contrast, for diffusion on all A clusters in the network, $R(t) \sim t^{1/d_w'}$ with $d_w' = 2d_w/(2 + d_f - d)$ (see e.g. [5]), and $P_0(t) - P_0(\infty)$ does *not* scale as $[R(t)]^{-d_t}$.

Above p_c, the correlation length ξ is the only characteristic length scale in the network, and the time $t_\xi \sim \xi^{d_w}$ the ant needs to explore the fractal labyrinths of size ξ is the only relevant time scale. Now, (2.2) holds only for times $t \ll t_\xi$. On large time scales $t \gg t_\xi$, corresponding to large length scales where the infinite percolation cluster is uniform, $P_0(t) - P_0(\infty) \sim t^{-d/2}$, similar to the behaviour in Euclidean lattices. The behaviour of $P_0(t)$ in both regimes can be bridged by the scaling ansatz

$$P_0(t) - P_0(\infty) = t^{-d_s'/2} f(t/t_\xi) \tag{2.3}$$

where $f(x) =$const for $x \ll 1$, and $f(x) \sim x^{-(d-d_s')/2}$ for $x \gg 1$. Using (2.3) in (2.1), it is easy to verify that the density of states $N(\omega)$ obeys, for $\omega > 0$, the scaling form

$$N(\omega) = \omega^{d_s'-1} g(\omega/\omega_\xi) \qquad \omega > 0 \tag{2.4}$$

where

$$\omega_\xi = t_\xi^{-1/2} \sim |p - p_c|^{\nu d_w/2} \tag{2.5}$$

is the characteristic frequency. For the scaling function one requires $g(x) =$ const for $x \gg 1$ where fractons occur [6] and $g(x) \sim x^{d-d_s'}$ for $x \ll 1$ where Debye phonons occur. The scaling form (2.4) has been suggested in [12], where it was assumed that (2.4) is valid for all ω. The constant term $P_0(\infty)$ in (2.3) gives rise to a delta function $\delta(\omega)$ in the density of states and, as a result, (2.4) obeys the normalization condition

$$\lim_{\epsilon \to 0+} \int_{\epsilon}^{\infty} d\omega N(\omega) = 1 - P_0(\infty). \tag{2.6}$$

Numerical studies of $N(\omega)$ have been performed for the infinite percolation cluster in two- and three-dimensional systems [14]. Here, we have extended these calculations to percolation networks as well, and have tested (2.4) for bond percolation on the square lattice. To obtain $N(\omega)$ we used the Williams–Maris technique [15]. Our numerical results shown in figure 1 support (2.4). The scaling function $g(x)$ in (2.4) is smooth near the crossover region, in agreement with previous numerical work [14] for the infinite percolation cluster.

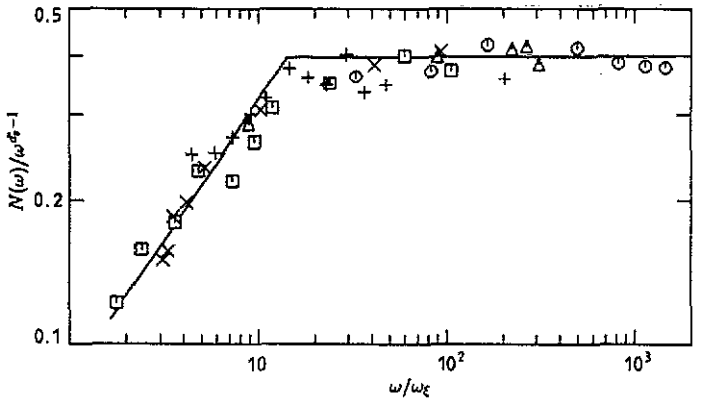

Figure 1. $N(\omega)/\omega^{d_f'-1}$ as a function of $\omega/(p-p_c)^{\nu d_w/2}$ to test the scaling behaviour of the density of states (2.4) above the percolation threshold $p_c = 1/2$, for bond-percolation networks on the square lattice. Different symbols correspond to different values of p: 0.52 (○), 0.54 (△), 0.55 (×), 0.56 (+), and 0.58 (□).

3. General two-component networks

Next we consider general AB mixtures, $h \geqslant 0$. It is useful to recall first the form of $N(\omega)$ for the two limiting cases $p = 0$ and $p = 1$. These are illustrated in figure 2 for the square lattice.

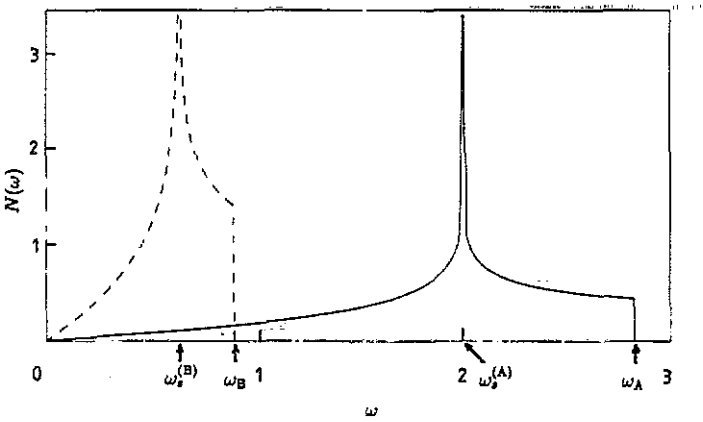

Figure 2. Density of vibrational states $N(\omega)$ against frequency ω in monatomic square lattices. For $p = 0$, a lattice of unit masses and spring constants f_B exists (broken curve), while for $p = 1$ a lattice of unit masses and force constants $f_A > f_B$ occurs (continuous curve). Vibrational modes occur below a cutoff frequency $\omega_B = (8f_B)^{1/2}$ for $p = 0$, and below a frequency $\omega_A = (8f_A)^{1/2}$ for $p = 1$. A singularity in $N(\omega)$ is present at frequencies $\omega_S^{(B)} = (4f_B)^{1/2}$ and $\omega_S^{(A)} = (4f_A)^{1/2}$, respectively. Both spectra are normalized to unity.

For $p = 1$, all lattice sites are connected by springs with force constants f_A, while for $p = 0$ all lattice sites are connected by springs with force constants f_B ($= hf_A$, $h \ll 1$). For $p = 0$, vibrational modes occur below the cutoff frequency (edge of the

spectrum)

$$\omega_B = (8f_B)^{1/2} \tag{3.1}$$

while for $p = 1$ vibrational modes occur below $\omega_A = (8f_A)^{1/2}$. Below the threshold frequencies, the density of states shows a singularity at $\omega_S^{(B)} = (4f_B)^{1/2}$ for $p = 0$, and at $\omega_S^{(A)} = (4f_A)^{1/2}$ for $p = 1$ [16]. For $h \ll 1$, the density of states of the ordered B lattice, $N_B(\omega)$, is located at frequencies well inside the Debye regime of the density of states of the ordered A lattice where $N_A(\omega) \cong (2\pi f_A)^{-1}\omega$. We expect that the frequencies $\omega_S^{(B)}$ and ω_B of (3.1), which are characteristic of the ordered B lattice, will also show up in the random *AB* network. At low concentrations of A bonds ($p \ll 1$), $N(\omega)$ is well described by the shape of $N_B(\omega)$, as long as $\omega < \omega_B$. Because of disorder, the singularity in $N_B(\omega)$ is smoothed out and becomes a 'hump' in $N(\omega)$ around $\omega_S^{(B)}$. For frequencies above ω_B, $N(\omega)$ exhibits a number of peaks representing localized lattice vibrations of small A clusters embedded in the B matrix [1].

The situation becomes more complex near and above p_c, where the infinite A cluster occurs. From figure 2 and section 2, it is intuitively clear that at p_c we can expect sound waves at very low frequencies, followed by a hump at $\omega_S^{(B)}$, and fracton like excitations above ω_B, for $h \ll 1$. The set-in of sound waves, however, is not simply determined by ω_B, but by a second characteristic frequency $\omega_h \ll \omega_B$ which depends on the ratio h (see below). Above p_c, the correlation length ξ is finite and consequently also ω_ξ (of 2.5) has to be taken into account.

To obtain $N(\omega)$ for p at p_c and above p_c, we consider the related random walk problem where f_A and f_B denote the transition rates along the A and B bonds. In the following we discuss two limiting cases: (I) $\omega_\xi \ll \omega_h \ll \omega_B$, and (II) $\omega_h \ll \omega_B \ll \omega_\xi$.

3.1. Frequency regime I: $\omega_\xi \ll \omega_h \ll \omega_B$

First we consider the random walk problem at p_c. In contrast to the case $h = 0$, a random walker (which in this case is often referred to as a 'termite') can perform jumps along both types of bonds. If the termite moves along the A bonds, it explores the fractal labyrinth of an A cluster, and attempts to leave the cluster, through B bonds, with a probability $\sim h \ll 1$. The transition rate f_A determines the mean jump time $t_A \sim f_A^{-1}$ along an A bond, which we take as the unit of time.

Along the B bonds, the mean jump time t_B is proportional to $h^{-1}t_A$, and the motion of the termite is slowed down considerably [17]. Accordingly, for very short times $t_A < t \ll t_B$ (corresponding to length scales $1 < r \ll h^{-1/d_w}$, where the length of a bond has been chosen as unity) diffusion is determined solely by the behaviour of the termite on the fractal labyrinths of A clusters, and $R(t) \sim t^{1/d_w'}$ as for random walks on standard percolation networks (section 2). Thus, from (2.2) we expect

$$P_0(t) - P_0(\infty) \sim t^{-d_s'/2} \qquad t_A \ll t \ll t_B. \tag{3.2}$$

For times $t > t_B$, the termite can move also along B bonds and explores both A and B clusters, which become thus coupled to each other. According to Hong *et al* [17], there exists a second characteristic time $t_h \sim f_A^{-1}\, h^{-\nu d_w \phi} \gg t_B$, above which diffusion becomes normal and $R(t) \sim (D_h\, t)^{1/2}$, with the diffusion constant $D_h \sim f_A\, h^{\mu\phi}$, where $\phi = (\mu + s)^{-1}$, and μ and s are the conductivity and the superconductivity exponents, respectively. For $t \gg t_h$, we then expect

$$P_0(t) \sim t^{-d/2} \qquad t \gg t_h \tag{3.3}$$

where now $P_0(\infty) = 0$, since the termite can diffuse everywhere in the network.

In previous publications on the termite problem [17], it has been assumed that t_h is the only characteristic time scale of the problem and a scaling theory for $R(t)$ based upon this assumption has been performed. As we have seen, this ansatz is not justified since for shorter times $t \ll t_h$, t_B is the relevant time scale, and anomalous diffusion occurs only for $t < t_B$, *not* for $t < t_h$ as assumed in [17].

In the equivalent vibrational problem, the anomalous behaviour of the random walk for times $t_A \ll t \ll t_B$, corresponds to fracton-like vibrations of the A-bonds in the network for frequencies $\omega_B \ll \omega \ll \omega_A$, as discussed qualitatively above. Accordingly, the density of states $N(\omega)$ should scale as

$$N(\omega) \sim \omega^{d_s'-1} \qquad \omega_B \ll \omega \ll \omega_A \tag{3.4}$$

where fractons occur.

The intermediate time regime $t_B < t < t_h$, in which the termite can explore both A and B clusters, corresponds to vibrations associated with both A and B springs in the network, for frequencies $\omega_h < \omega < \omega_B$. The characteristic frequency corresponding to t_h,

$$\omega_h \sim f_A^{1/2} h^{\nu d_w \phi/2} \tag{3.5}$$

determines the frequency scale below which Debye phonons should occur, and

$$N(\omega) \sim \omega^{d-1} \qquad \omega \ll \omega_h. \tag{3.6}$$

The exponent $\nu d_w \phi/2$ in (3.5) is greater than $1/2$ and hence $\omega_h < \omega_S^{(B)} < \omega_B$. Accordingly, we expect that in this intermediate frequency regime, non-Debye phonons can be excited which manifest themselves by the hump in $N(\omega)$. Numerical calculations of $N(\omega)$ for two-dimensional bond–percolation networks at criticality support (3.4) and (3.6), as shown in figure 3.

The scaling behaviour of $N(\omega)$ is different from that in the case $h = 0$ (see (2.4)), because of the existence of two characteristic frequencies, ω_h of (3.5) and ω_B of (3.1). Outside the hump region, i.e. for $\omega < \omega_h$ or $\omega > \omega_B$, the following scaling form holds

$$N(\omega) \cong \omega^{d_s'-1}\, G(\omega/\omega_h) \tag{3.7}$$

where $G(x) \sim$ const for $\omega > \omega_B$, and $G(x) \sim x^{d-d_s'}$ for $x \ll 1$. The results of numerical simulations are plotted in figure 4 (*a*). The data collapse supports our ansatz (3.7).

If we consider all frequencies, including those in the hump region, we obtain the results shown in figure 4 (*b*). Clearly, there is data collapse (scaling) for $\omega < \omega_h$ and $\omega > \omega_B$. Notice, however, that the data also collapse *above* ω_h for frequencies below the hump frequency, $\omega < \omega_S^{(B)}$. This data collapse can be identified with the one obtained for the termite problem for times $t_B \ll t < t_h$ at $p = p_c$ (see figure 10 of Hong *et al* [17]).

For $p > p_c$, the above results hold if $h^\phi \gg (p - p_c)$. This condition means that the time t_h the termite needs to explore large length scales in the system, is much smaller than the time t_ξ that would take the termite to move over length scales of order ξ on the infinite A cluster alone. The condition $t_\xi \gg t_h$ corresponds to frequencies $\omega_\xi \ll \omega_h$ (see figure 5). In this limit, t_ξ is irrelevant and t_B and t_h represent the only characteristic times in the system. Equivalently, ω_B and ω_h represent the only characteristic frequencies.

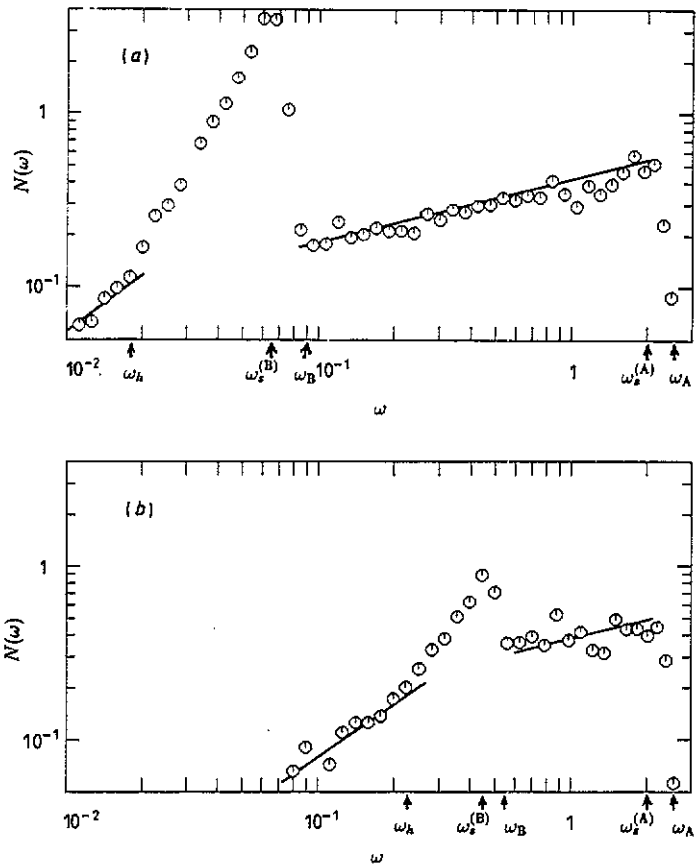

Figure 3. Density of vibrational states for bond-percolation networks at the critical concentration $p_c = 1/2$, for several ratios of spring constants: (*a*) $h = 10^{-3}$, and (*b*) 0.05. The positions of ω_h, $\omega_S^{(B)}$, ω_B, $\omega_S^{(A)}$ and ω_A are indicated by arrows. The straight lines display the slopes predicted by the theory (equations (3.4) and (3.6)).

3.2. *Frequency regime II:* $\omega_h \ll \omega_B \ll \omega_\xi$

This regime corresponds to the case $t_\xi \ll t_B$. Within the 'short' time regime $t < t_B$, the walker can explore length scales of the order of the correlation length ξ, thus escaping from the fractal labyrinth of the infinite A cluster *before* exiting the infinite cluster through B bonds. In this limit, the random walker behaves essentially as the ant in the labyrinth of section 2 [17], and $P_0(t)$ is expected to obey (2.3). Nothing special can occur for times $t \geqslant t_B$ since the walker has already explored large length scales when it can transit through B bonds.

In the corresponding vibrational problem, the standard crossover from fractons to Debye phonons occurs at the characteristic frequency $\omega_\xi \gg \omega_B$. Now, vibrations associated with the B sublattice occur at frequencies well inside the Debye-phonon regime of the A network. In contrast to the smooth behaviour of $P_0(t)$ near t_B, the existence of the second frequency ω_B in $N(\omega)$ is manifested by the hump at $\omega_S^{(B)}$, which appears as a low-frequency peak (see also [18]). Thus, the density of states

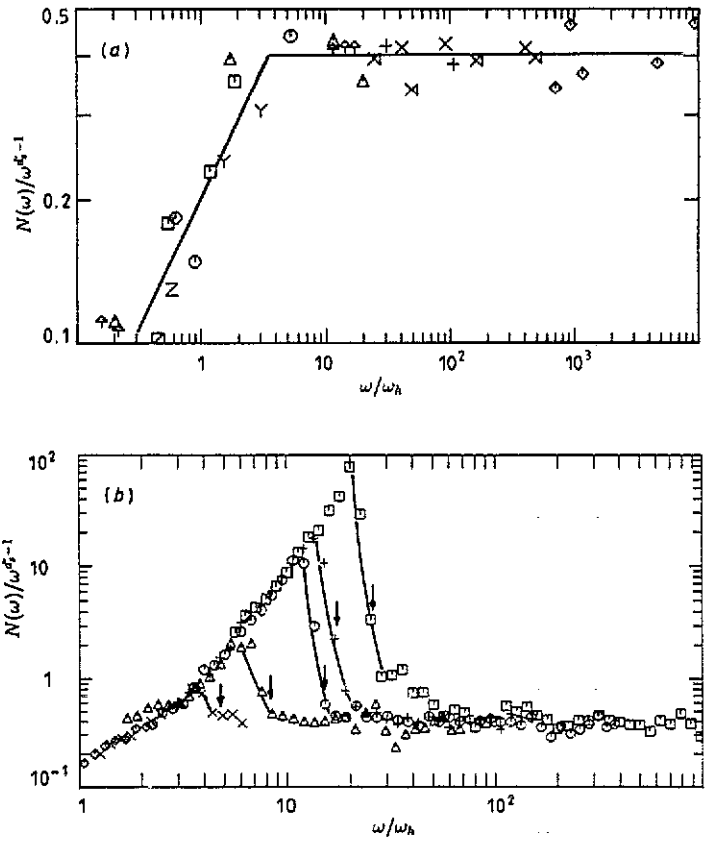

Figure 4. Test of the scaling behaviour of the density of states (3.7), for bond-percolation networks in two dimensions at the percolation threshold p_c, for several values of h. (*a*) Debye regime, excluding the region of the hump, for: $10^{-6} \leqslant h \leqslant 0.1$, on 400 x 400 lattices and averages over 10 system realizations each. (*b*) All frequencies, including the hump region, for: $10^{-4} \leqslant h \leqslant 0.1$, where the arrows indicate the values of ω_B/ω_h, on 100 x 100 lattices and averages over 50 system realizations each.

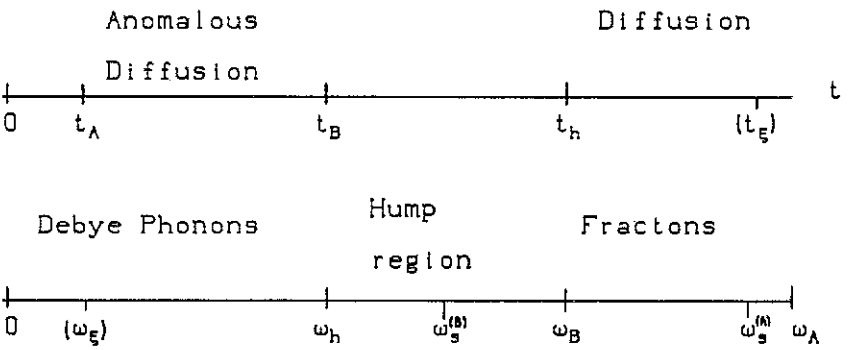

Figure 5. (*a*) Schematic representation of different time regimes for random walks on random AB networks, with two types of bonds representing mean jump times t_A and $t_B > t_A$, near the critical concentration of A with $t_B < t_h \ll t_\xi$. (*b*) The corresponding frequency regimes of the related vibrational problem, where generically, $\omega_* \sim t_*^{-1/2}$.

should behave as in (2.4) for frequencies $\omega \gg \omega_B$, i.e.

$$N(\omega) \cong \omega^{d_f'-1}\, g(\omega/\omega_\xi) \qquad \omega \gg \omega_B \tag{3.8}$$

and fractons occur at $\omega \gg \omega_\xi$, with a 'smooth' crossover to Debye phonons for $\omega \ll \omega_\xi$. We show in figure 6 illustrative examples of the density of states obtained for $\omega_B < \omega_\xi$. Values of $N(\omega)$ for $\omega \gg \omega_B$ are indistinguishable from those obtained for the same p when $h = 0$, thus supporting our ansatz (3.8).

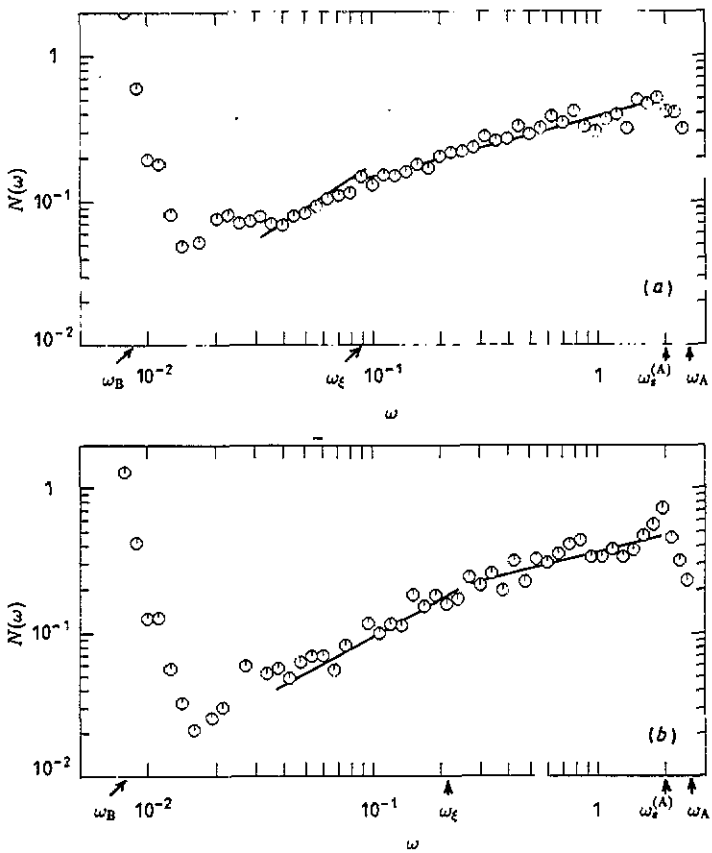

Figure 6. Same as in figure 3, for $p > p_c$ and $\omega_\xi \gtrsim \omega_B$, with $h = 10^{-5}$: (*a*) p=0.57 and (*b*) p=0.60. The positions of ω_B, ω_ξ, $\omega_S^{(A)}$ and ω_A are indicated by arrows. The straight lines display the slopes predicted by the theory (equations (2.4) and (3.8)).

Because of normalization, the amplitude of the B hump around $\omega_S^{(B)}$ grows as f_B decreases. When $f_B = 0$, the B sublattice contributes to $N(\omega)$ a delta-like function at $\omega = 0$, and (3.8) holds for all frequencies $\omega > 0$, as discussed in section 2.

4. Summary and concluding remarks

We have studied scalar vibrational properties of random two-component networks, where two types of harmonic springs, f_A and $f_B = hf_A$ ($h \ll 1$) are present with

probability p and $1-p$, respectively. We have developed a scaling theory for the density of states $N(\omega)$ near the critical concentration p_c, and have tested it by numerical simulations on the square lattice.

A salient feature of the present model is the manifestation of a 'hump' in $N(\omega)$, representing non-Debye phonons near the maximum vibrational frequency of the B sublattice, $\omega_B \sim f_B^{1/2}$. For $p > p_c$ and h sufficiently small, the standard fracton–phonon crossover is recovered at a characteristic frequency $\omega_\xi \gg \omega_B$, which is determined by the correlation length ξ. For finite h and p sufficiently close to p_c, a new type of fracton–phonon crossover is obtained which is determined by two characteristic frequencies: ω_h (which depends on h) and ω_B, with $\omega_h \ll \omega_B$. The hump mediates the crossover from fracton-like modes (occurring for $\omega \gg \omega_B$), to Debye phonons (occurring for $\omega \ll \omega_h$) when $\omega_h \gg \omega_\xi$.

Similar qualitative behaviour of the density of states can be expected for simple cubic lattices where a hump in $N(\omega)$, originating from the maximum in the density of states of the ordered B lattice, is also present near the critical concentration $p_c \cong 0.2492$ (see, e.g. [1]).

Acknowledgments

We have highly benefited from discussions with S. Havlin who pointed out to us the role of the finite clusters in (3.2) leading to $P_0(\infty)$. We gratefully acknowledge financial support by the Deutsche Forschungsgemeinschaft.

References

[1] Dean P 1972 *Rev. Mod. Phys.* **44** 127
[2] Stauffer D 1985 *Introduction to Percolation Theory* (London: Taylor and Francis)
Havlin S and Bunde A 1991 *Fractals and Disordered Systems* ed A Bunde and S Havlin (Heidelberg: Springer Verlag)
Mandelbrot B B 1982 *The Fractal Geometry of Nature* (San Francisco: Freeman)
[3] Alexander S and Orbach R 1982 *J. Physique Lett.* **43** L625
[4] Gefen Y, Aharony A and Alexander S 1983 *Phys. Rev. Lett.* **50** 77
[5] Havlin S and Ben-Avraham D 1987 *Adv. Phys.* **36** 695
[6] Alexander S, Laermans C, Orbach R and Rosenberg H M 1983 *Phys. Rev.* B **28** 4615
[7] For recent reviews see, e.g.,
Courtens E, Vacher R and Stoll E 1989 *Physica* D **38** 41
Kjems J K 1991 *Fractals and Disordered Systems* ed A Bunde and S Havlin (Heidelberg: Springer Verlag)
[8] It appears, however, that the assumption of scalar elasticity for silica aerogels does not hold for all frequencies, and a second crossover due to bending elasticity (see [9]) occurs in these tenuous materials:
Vacher R *et al* 1990 *Phys. Rev. Lett.* **65** 1008
[9] Feng S 1985 *Phys. Rev.* B **32** 5793
[10] Caciuffo R, Francescangeli O, Melone S, Stefanon M, Gering E, Suck J–B, Bonnet M, Allia P and Vinai F 1989 *J. Phys.: Condens. Matter* **1** 5621
[11] Carini G, Cutroni M, Fontana A, Mariotto G and Rocca F 1984 *Phys. Rev.* B **29** 3567
[12] Aharony A, Alexander S, Entin-Wohlman O and Orbach R 1985 *Phys. Rev.* B **31** 2565
[13] Alexander S 1983 *Percolation Structures and Processes, Ann. Israel Phys. Soc.* **5** ed G Deutsche, R Zallen and J Adler (Bristol: Adam Hilger)
Alexander S, Bernasconi J, Schneider W and Orbach R 1981 *Rev. Mod. Phys.* **53** 175
[14] Grest G S and Webman I 1984 *J. Physique Lett.* **45** L1155

Yakubo K and Nakayama T 1989 *Phys. Rev.* B **40** 517
[15] Williams M L and Maris H J 1985 *Phys. Rev.* B **31** 4508
[16] Bowers W A and Rosenstock H B 1950 *J. Chem. Phys.* **18** 1056
[17] Hong D C, Stanley H E, Coniglio A and Bunde A 1986 *Phys. Rev.* B **33** 4564
See also Straley J 1990 *Phys. Rev.* B **41** 9340
[18] Burton D, Dow R C M and Lambert C J 1986 *Phys. Rev.* B **33** 7803